Beam-quality and guiding-magnetic-field requirements for a high-power traveling-wave amplifier operating at 35 GHz

L. Schächter
Electrical Engineering Department, Technion, Israel Institute of Technology, Haifa 32000, Israel

J. A. Nation
School of Electrical Engineering, Cornell University, Ithaca, New York 14853
(Received 7 August 1997; revised manuscript received 2 February 1998)

A two-dimensional quasianalytic model has been developed for the investigation of the performance of a high-efficiency traveling-wave amplifier operating at 35 GHz. Simulations indicate that a relative energy spread of less than 5% is sufficient to reach high efficiency. It is also shown that there is an optimal guiding magnetic field for a given geometry of the slow-wave structure. [S1063-651X(98)11206-0]

PACS number(s): 41.75.Fr

INTRODUCTION

The next linear collider (NLC) will require acceleration gradients in excess of 100 MV/m. The lower limit of the necessary gradient is achievable with the *X*-band klystrons as developed at Stanford Linear Accelerator Center (SLAC) [1]. For higher gradients (>200 MV/m) the source will have to operate at a higher frequency. The obvious question is what should be the operation frequency of the future system. There is no optimal value which can be established from a single or simple criterion. The complexity of the analysis and the variety of criteria involved were discussed more than ten years ago by Palmer [2], who concluded that a good tradeoff is operation close to 14.5 GHz. More recently Wilson [3] has analyzed the requirements of a 5–15 TeV accelerator and the conclusion was in favor of operation at 34 GHz. However, higher energies would require even higher operating frequencies.

The spectrum of possibilities, with regard to what rf source should be utilized, is quite limited if we assume that conceptually NLC will operate in a similar way as the Stanford Linear Collider (SLC). One possibility is to scale the present *klystron* technology to 35 GHz. This may prove to be a difficult approach since the diameter of the drift tube between cavities has to be scaled down according to the frequency increase, in order to keep the waveguide below cutoff for all electromagnetic modes. At the same time the current in the electron beam has to be comparable to that in present day klystrons and therefore the propagation of the electron beam imposes severe constraints on the guiding magnetic field. Furthermore, the closer the beam is to the external wall, the larger the variation of the rf field across the beam, consequently affecting the efficiency of the system. To avoid these difficulties the beam radius is expected to be one order of magnitude smaller than the vacuum wavelength (i.e., $R_{\mathrm{beam}}\sim\lambda/8$ [3]). In spite of these constraints the klystron may still have a significant contribution to the next generation of accelerators. In fact Wilson [3] indicates that since most of the difficulties of the klystron arise from its pencil beam, the alternative, namely, a sheet beam, [4] may eliminate many of the obstacles.

A second possibility is the *gyrotron* which is under intensive investigation at the University of Maryland [5]. It has inherent advantages over all other rf sources at high frequency with regard to continuous operation at high power levels. However, the presence of lossy materials required for the massive mode suppression may become an obstacle in obtaining an overall high efficiency. An interesting concept which utilizes the advantages of the klystron at low frequency and these of the gyrotron at high frequency is being developed by Hirshfield and co-workers [6]. It relies on conversion of low-frequency power from a regular klystron by bunching an electron beam which in turn generates, after being isolated from the input rf, a higher harmonic of the input frequency. The conversion mechanism is similar to that which occurs in a gyrotron. Obviously the constraints on this conversion scheme with regard to efficiency are high since the overall efficiency is the product of that of the converter and the klystron.

The third possibility is to exploit the advantages of a *traveling-wave* amplifier and this will be the topic of this theoretical study. As an acceleration structure, the traveling-wave amplifier consists of a disk-loaded waveguide but contrary to an acceleration structure where the aperture's diameter has to be reduced according to the increase in the operating frequency, in this case (35 GHz) the aperture may be comparable to the dimensions required in an *X*-band structure. In this way we have eliminated one major constraint which is unavoidable in a pencil-beam klystron. The price we pay for using at 35 GHz the same disk aperture as in an *X*-band structure is operation at relatively high group velocity and low interaction impedance. The latter has two effects: for a given current and for maximum efficiency it makes the required interaction length longer, which leads to a higher sensitivity to beam quality. On the other hand, it makes the transverse motion of the particles less ''violent,'' in this way reducing the probability of particles hitting the structure's wall at a given guiding magnetic field.

In addition to the iris aperture, which has not been reduced in the present design (35 GHz), the amount of current carried by the beam remains of the same order of magnitude (as in the *X*-band case) implying that a typical guiding mag-

netic field of 0.5 T will be required. This field corresponds to a cyclotron frequency $f_c \equiv eB/2\pi m\gamma$ of 14 GHz (assuming $\gamma=2$) and for sufficiently low velocities, the electrons may enable a ''gyrotronlike'' interaction to occur, namely, $|\omega - kV| = \omega_c$ (where k is the wave number in the structure). Consequently we may expect severe reduction of the efficiency and electron interception by the structure. The problem may become even more severe in a permanent periodic magnetic field (PPM) since the latter acts as a wiggler and the radial oscillation may become even larger comparing to a uniform magnetic field.

In this study we investigate several aspects associated with the operation of a high-power single-stage traveling-wave amplifier at 35 GHz. For this purpose we have developed a quasianalytic two-dimensional (2D) model of the interaction of an ensemble of electrons with a *symmetric* transverse magnetic (TM) mode. The interaction occurs with all the components of the electromagnetic field and not only the longitudinal electric field as is the case in a 1D model [7–9]. First, we compare the performance of two similar amplifiers, one operating at 35 GHz and the other at X band. We show that the sensitivity of the former to beam quality is higher but its operation is definitely feasible. Secondly, we investigate the effect of the guiding field on the interaction of a slow wave with an ideal beam, and thirdly, we show that optimal disk aperture and optimal guiding magnetic field do exist. This quasianalytic 2D model is adequate for simulation of the interaction in a two-stage amplifier which based on our experience in X band should enable generation of radiation with higher efficiency. The latter is a crucial requirement for a rf source designed to feed an acceleration module.

DYNAMICS OF THE SYSTEM

An electromagnetic wave is injected into a disk-loaded periodic structure and it interacts with a pencil electron beam. Assuming for the moment that the structure is uniform, then in the vicinity of the axis the dominant electromagnetic field components of the TM mode are assumed to be given by

$$\begin{aligned} E_z(r,z;t) &= E_0 I_0(\Gamma r)\cos(\omega t - kz - \psi), \\ E_r(r,z;t) &= -\gamma_{\rm ph} E_0 I_1(\Gamma r)\sin(\omega t - kz - \psi), \\ H_\phi(r,z;t) &= -\frac{1}{\eta_0}\,\gamma_{\rm ph}\beta_{\rm ph} E_0 I_1(\Gamma r)\sin(\omega t - kz - \psi). \end{aligned} \tag{1}$$

In these expressions k is the wave number which is assumed to correspond to a phase velocity smaller than c; $\Gamma \equiv \sqrt{k^2-(\omega/c)^2}$. The normalized phase velocity is denoted by $\beta_{\rm ph} \equiv \omega/ck$, $\gamma_{\rm ph} \equiv 1/\sqrt{1-\beta_{\rm ph}^2}$, and $\eta_0 \equiv \sqrt{\mu_0/\epsilon_0}$. It will be shown in the last section that radial oscillations of the beam envelope are relatively small, therefore we neglect the coupling of the TM to TE mode throughout this analysis.

In addition to the rf field there is a guiding magnetic field B_0 which is assumed to be uniform. In the absence of the radiation field we may assume that the electron beam injected in the system is uniformly distributed in the radial as well as in the longitudinal direction. Its density, denoted by n_0, generates an electrostatic field which in turn affects the motion of each electron; this field is given by

$$E_r^{(\rm dc)}(r \leqslant R_{\rm beam}) = -\frac{en_0}{2\epsilon_0}\, r. \tag{2}$$

Furthermore, since the average velocity of the beam is v_0 the magnetic field associated with this motion in the beam domain is given by

$$\mu_0 H_\phi^{(\rm dc)}(r \leqslant R_{\rm beam}) = -v_0\,\frac{en_0}{2\epsilon_0 c^2}\, r. \tag{3}$$

Transverse motion. From these expressions we can readily determine the radial equation of motion of the ith electron; it is given by

$$\begin{aligned} &\frac{d}{dt}\left(\gamma_i \frac{dr_i}{dt}\right) - \gamma_i r_i\left(\frac{d\phi_i}{dt}\right)^2 + \omega_c r_i \frac{d\phi_i}{dt} - \frac{\omega_p^2}{2\gamma_i^2}\, r_i \\ &\quad = -\frac{e}{m}\,(E_r - v_z B_\phi), \end{aligned} \tag{4}$$

where $\omega_c \equiv eB_0/m$ is the cyclotron angular frequency and $\omega_p \equiv \sqrt{e^2 n_0/m\epsilon_0}$ is the plasma angular frequency. The components of the TM mode have no contribution to the azimuthal force therefore the azimuthal equation of motion reads

$$\frac{d\gamma_i}{dt}\, r_i \frac{d\phi_i}{dt} + 2\gamma_i \frac{dr_i}{dt}\frac{d\phi_i}{dt} + \gamma_i r_i \frac{d^2\phi_i}{dt^2} - \omega_c \frac{dr_i}{dt} = 0. \tag{5}$$

Assuming that the guiding magnetic field is *uniform*, this last expression can be simplified by multiplying by the radius where the ith particle is located (r_i). The result is the conservation of angular momentum, i.e.,

$$\frac{d}{dt}\left[r_i^2\left(\gamma_i \frac{d\phi_i}{dt} - \frac{\omega_c}{2}\right)\right] = 0. \tag{6}$$

The latter can now be integrated by further assuming that when created, the *azimuthal* motion of the electron is zero, i.e.,

$$\frac{d\phi_i}{dt} = 0, \tag{7}$$

which imposes the azimuthal angular frequency at all times

$$\frac{d\phi_i}{dt} = \frac{\omega_c}{2\gamma_i r_i^2}\,[r_i^2 - r_{i,\rm in}^2], \tag{8}$$

where $r_{i,\rm in}$ is the radius where the electron was created. The result presented here corresponds to either the dynamics of an electron generated on an immersed cathode or when beam compression is utilized, to the dynamics of electrons outside the diode gap—assuming that in the compression process no azimuthal motion develops ($B \| E$ in the diode). In case Eq. (7) is not satisfied ($d\phi_{i,\rm in}/dt \neq 0$) we can still bring Eq. (9) to the same form by replacing $r_{i,\rm in} \rightarrow r_{i,\rm in}^{(\rm eff)} \equiv r_{i,\rm in}[1 - 2\gamma_{i,\rm in}(d\phi_{i,\rm in}/dt)(1/\omega_c)]^{1/2}$.

With the azimuthal motion established in Eq. (8) we can write an expression for the radial equation of motion which is dependent only on the radial coordinate:

$$\frac{d}{dt}\left(\gamma_i \frac{dr_i}{dt}\right)+\frac{\omega_c^2}{4\gamma_i r_i^3}[r_i^4-r_{i,\mathrm{in}}^4]-\frac{1}{2\gamma_i^2}\omega_p^2 r_i$$
$$=-\frac{e}{m}(E_r-v_z B_\phi)_i$$
$$=\frac{e}{m}\gamma_{\mathrm{ph}}(1-\beta_{\mathrm{ph}}\beta_{z,i})E_0 I_1(\Gamma r_i)\sin[\omega t-kz_i(t)-\psi]. \quad (9)$$

Equation (9) determines the transverse motion of the electrons in the presence of the given electromagnetic field.

Longitudinal motion. Parallel to the axis of the structure the equation of motion is given by

$$\frac{d}{dt}(\gamma_i\beta_{z,i})=-\frac{e}{mc}(E_z+v_r\mu_0 H_\phi)_i$$
$$=-\frac{e}{mc}E_0 I_0(\Gamma r_i)\cos[\omega t-kz_i(t)-\psi]$$
$$+\frac{e}{mc}E_0\beta_{r,i}\gamma_{\mathrm{ph}}I_1(\Gamma r_i)\sin[\omega t-kz_i(t)-\psi]. \quad (10)$$

Note that the radial velocity ($c\beta_{r,i}$) together with the azimuthal magnetic rf field (H_ϕ) has a nonzero contribution to the longitudinal force.

Poynting theorem. After establishing the equations which determine the dynamics of the particles we shall consider its effect on the dynamics of the rf field. The macroscopic current density in terms of the particle dynamics is given by

$$J_r(r,z;t)=-e\sum_i v_{r,i}\frac{1}{2\pi r}\delta[r-r_i(t)]\delta[z-z_i(t)], \quad (11)$$
$$J_z(r,z;t)=-e\sum_i v_{z,i}\frac{1}{2\pi r}\delta[r-r_i(t)]\delta[z-z_i(t)].$$

Thus bearing in mind that the system operates in steady state and assuming that it remains in a linear regime at all times, the average power exchange is determined by

$$\frac{d}{dz}\langle P(z)\rangle_t=-\int_{\mathrm{CS}} da\langle \mathbf{J}\cdot\mathbf{E}\rangle_t, \quad (12)$$

where the integration is over the cross section (CS) of the waveguide and $\langle P(z)\rangle_t\equiv\langle\int_{\mathrm{CS}} da S_z\rangle_t$. At this point we introduce the concept of the interaction impedance which relates the average power which flows in the system with the longitudinal electric field on axis

$$\langle P(z)\rangle_t=\frac{1}{2}\frac{E_0^2(\pi R_{\mathrm{int}}^2)}{Z_{\mathrm{int}}}, \quad (13)$$

where R_{int} is the internal radius of the disk-loaded structure. We shall prefer this definition of the interaction impedance over Pierce's $[P=E_0^2/2Z_{\mathrm{int}}k^2]$ since in high-efficiency devices the structure has to be tapered and the phase velocity varies in space. In such a case it is possible to keep R_{int} constant and change the other geometric parameters. Consequently, the definition in Eq. (13) is more convenient.

We now proceed by substituting in Eq. (12) the last expression: the result is

$$\frac{d}{dz}\left[\frac{1}{2}\frac{E_0^2\pi R_{\mathrm{int}}^2}{Z_{\mathrm{int}}}\right]=-2\pi\int_0^{R_{\mathrm{int}}}dr r\frac{1}{T}\int_0^T dt$$
$$\times\sum_i\frac{-e}{2\pi r}\delta[r-r_i(t)]$$
$$\times\delta[z-z_i(t)][v_{z,i}I_0(\Gamma r)$$
$$\times\cos(\omega t-kz-\psi)-v_{r,i}\gamma_{\mathrm{ph}}I_1(\Gamma r)$$
$$\times\sin(\omega t-kz-\psi)]. \quad (14)$$

The integration over time and radius becomes trivial due to the presence of the δ functions thus denoting by N the number of particles in one period of the wave (T) we obtain

$$\frac{d}{dz}E_0^2(z)=\frac{2Z_{\mathrm{int}}}{\pi R_{\mathrm{int}}^2}\frac{eN}{T}E_0(z)\left\langle I_0[\Gamma r_i(z)]\right.$$
$$\times\cos[\omega\tau_i(z)-kz-\psi(z)]$$
$$-\frac{\beta_{r,i}}{\beta_{z,i}}\gamma_{\mathrm{ph}}I_1[\Gamma r_i(z)]$$
$$\left.\times\sin[\omega\tau_i(z)-kz-\psi(z)]\right\rangle_i. \quad (15)$$

In this expression two assumptions have been made: (i) the effect of the particles on the rf field is to cause spatial variations (of the amplitude and phase) only in the z direction and, (ii) rather than following the particles in time, we follow them in space; thus $\tau_i(z)$ represents the time the ith particle reaches the point z and $r_i(z)$ is the radial location of the same particle at z.

We proceed by identifying the average current in one period of the wave as $I\equiv eN/T$ and resorting to complex notation $\bar{E}_0\equiv E_0 e^{-j\psi}$. With this notation the dynamics of the complex amplitude of the rf field is given by

$$\frac{d}{dz}\bar{E}_0(z)=\frac{IZ_{\mathrm{int}}}{\pi R_{\mathrm{int}}^2}\left\langle\left\{I_0[\Gamma r_i(z)]\right.\right.$$
$$\left.\left.-j\frac{\beta_{r,i}}{\beta_{z,i}}\gamma_{\mathrm{ph}}I_1[\Gamma r_i(z)]\right\}e^{-j\chi_i(z)}\right\rangle_i, \quad (16)$$

$$\frac{d}{dz}\chi_i(z)=\frac{\omega}{c\beta_{z,i}}-k,$$

where $\chi_i(z)$ is the phase of the ith particle relative to the wave. In the first expression the second term can be neglected since for most practical purposes

$$|\beta_{r,i}|\,\gamma_{\rm ph} \ll \beta_{z,i} \tag{17}$$

thus

$$\frac{d}{dz}\,\overline{E}_0(z)=\frac{IZ_{\rm int}}{\pi R_{\rm int}^2}\,\langle I_0[\Gamma r_i(z)]e^{-j\chi_i(z)}\rangle_i\,,$$

$$\frac{d}{dz}\,\chi_i(z)=\frac{\omega}{c\beta_{z,i}}-k. \tag{18}$$

The term $IZ_{\rm int}$ in the first equation is the product of a beam term (I) and an electromagnetic term ($Z_{\rm int}$). It is this product which controls the *coupling* of the beam with the wave. Furthermore, in Eq. (18) we have assumed that the transverse motion does not affect directly the amplitude of the field, however, it may affect it significantly in an indirect way via the phase as will be shown subsequently. In the framework of the same approximation we may write for the single particle energy conservation the expression

$$\frac{d}{dz}\,\gamma_i(z)=-\frac{1}{2}\,\frac{e}{mc^2}\,\{\overline{E}_0(z)I_0[\Gamma r_i(z)]e^{j\chi_i(z)}+\text{c.c.}\}. \tag{19}$$

This is related to the transverse and longitudinal velocities by

$$\gamma_i\equiv[1-\beta_{z,i}^2-\beta_{r,i}^2-\beta_{\phi,i}^2]^{-1/2}. \tag{20}$$

Substituting Eq. (8) and defining

$$\gamma_{z,i}\equiv\frac{1}{\sqrt{1-\beta_{z,i}^2}}\quad\text{or}\quad\beta_{z,i}=\sqrt{1-\gamma_{z,i}^{-2}} \tag{21}$$

we obtain

$$\gamma_{z,i}=\frac{\gamma_i}{\sqrt{1+(\gamma_i\beta_{r,i})^2+[\omega_c(r_i^2-r_{i,\rm in}^2)/2cr_i]^2}}, \tag{22}$$

that clearly reveals the relation between phase dynamics [Eq. (18)], the guiding magnetic field, and the transverse motion.

In order to summarize the equations that describe the dynamics of the system it is convenient to introduce a series of normalized variables. We start by assuming that the interaction length is d, which allows us to determine the normalized coordinate $\zeta=z/d$ and normalized field amplitude $a=e\overline{E}_0 d/mc^2$. Based on these definitions the normalized coupling coefficient is

$$\alpha\equiv\frac{IZ_{\rm int}}{mc^2/e}\,\frac{d^2}{\pi R_{\rm int}^2}. \tag{23}$$

Further we define $\Omega=\omega d/c$, $K=kd$, $\Omega_c=ecBd/mc^2$, and

$$\Omega_p^2\equiv\frac{eI\eta_0}{mc^2}\,\frac{d^2}{\pi R_{\rm beam}^2}\,\frac{1}{\langle\beta_{z,i}\rangle_i}. \tag{24}$$

$R_{\rm beam}$ is the beam radius. Based on the argument of the modified Bessel functions it is convenient to define $\overline{r_i}=\omega r_i/c\gamma_{\rm ph}\beta_{\rm ph}$ and correspondingly, $\overline{p_{r,i}}=\gamma_i\beta_{r,i}\Omega/\gamma_{\rm ph}\beta_{\rm ph}$. With these definitions we are now in position to summarize the equations which describe the dynamics of the system; these read

$$\begin{aligned}
&\frac{d}{d\zeta}\,a=\alpha\langle I_0(\overline{r_i})e^{-j\chi_i}\rangle_i\,,\\
&\frac{d}{d\zeta}\,\chi_i=\Omega(\beta_{z,i}^{-1}-\beta_{\rm ph}^{-1}),\\
&\frac{d}{d\zeta}\,\gamma_i=-\frac{1}{2}\,[aI_0(\overline{r_i})e^{j\chi_i}+\text{c.c.}],\\
&\frac{d}{d\zeta}\,\overline{r_i}=\overline{p}_{r,i}/\gamma_i\beta_{z,i}\,,\\
&\frac{d}{d\zeta}\,\overline{p}_{r,i}=\Omega_c^2(\overline{r_i^4}-\overline{r_{i,\rm in}^4})/4\gamma_i\beta_{z,i}\overline{r_i^3}+\overline{r_i}\Omega_p^2/2\beta_{z,i}\gamma_i^2\\
&\qquad-\frac{1}{2}\,(jae^{j\chi_i}+\text{c.c.})I_1(\overline{r_i})\Omega(1-\beta_{z,i}\beta_{\rm ph})/\beta_{z,i}\beta_{\rm ph}\,,\\
&\beta_{z,i}=(1-\gamma_i^{-2}-(\gamma_{\rm ph}\beta_{\rm ph}/\Omega\gamma_i)^2\{\overline{p_{r,i}^2}+[\Omega_c(\overline{r_i^2}\\
&\qquad-\overline{r_{i,\rm in}^2})/2\overline{r_i}]^2\})^{1/2}.
\end{aligned} \tag{25}$$

Before we proceed to examine the dynamics of the system as modeled by this set of equations it is instructive to evaluate the parameters for some typical parameters: consider a system which is 20 cm long driven by a 200 A, 500 kV, 6 mm diameter electron beam. This beam is guided by a 0.5 T magnetic field and typically 20 kW of 35 GHz rf power is injected into a structure of 100 Ω interaction impedance. The aperture of the disk is 12 mm in diameter. For these parameters $\alpha=13.8$, $\Omega_c=59$, $\Omega_p^2=243$, $\Omega=147$, $\gamma=1.98$, $I_0[\max(\overline{r_i})]=1.5$, and $I_1[\max(\overline{r_i})]=0.8$. Two main figures of merit are worth emphasis here: the relativistic plasma frequency $\Omega_p^2/\gamma^3\sim30$ is one order of magnitude smaller than the relativistic cyclotron frequency $\Omega_c^2/\gamma^2\sim900$. This ratio indicates that in zero order the electron beam is well confined by the magnetic field. The other figure of merit is the gain assuming 1D (longitudinal motion) and that all particles are located at one radial location $[\max(\overline{r_i})]$; this gain is $\simeq20.0\log_{10}(\frac{1}{3}\exp\{(\sqrt{3}/2)[\frac{1}{2}\alpha\Omega\langle I_0^2(\max(\overline{r_i})/(\gamma_i\beta_i)^3\rangle_i]^{1/3}\})=48$ dB (see Ref. [10], pp. 141 and 161). For comparison, if all particles are assumed to be on axis then the gain is 35 dB.

RESULTS AND DISCUSSION

The first step when investigating the operation of a traveling-wave amplifier at 35 GHz is to compare its performance with that of an X-band system. For simplicity at this stage we shall assume that an intense guiding field is applied such that we may confine our analysis to 1D motion. Adequate comparison requires that the beam is identical [500 kV, 200 A, 3 mm radius] in both cases. By virtue of energy conservation

$$\frac{d}{d\zeta}\left[\langle\gamma_i\rangle_i+\frac{|a|^2}{2\alpha}\right]=0, \tag{26}$$

the input power in the two cases has to be the same; the latter is assumed to be $P_{\rm in}=20$ kW and phase velocity equal to the average velocity of the electrons. At this point we have two options: either we require that the relative change of the wave number is the same, i.e.,

$$\frac{\mathrm{Im}(k)}{\mathrm{Re}(k)}=\frac{\sqrt{3}}{2}\left[\frac{1}{2}\frac{\alpha}{\Omega^2}\left\langle\frac{\beta_{\rm ph}^3}{(\gamma_i\beta_i)^3}\right\rangle_i\right]^{1/3}, \tag{27}$$

or that the overall gain is the same, namely,

$$\mathrm{Im}(kd)=\frac{\sqrt{3}}{2}\left[\frac{1}{2}\,\alpha\Omega\left\langle\frac{1}{(\gamma_i\beta_i)^3}\right\rangle_i\right]^{1/3}. \tag{28}$$

Since both the power in the beam and rf are the same at the input in both cases, we would obviously prefer to examine the two devices such that their output power (i.e., efficiency) will be the same. Consequently we prefer the criterion in Eq. (28) rather than that in Eq. (27).

By imposing the identical output power requirement [Eq. (28)] in both systems we enforce the following relation between the length and the interaction impedance of the two systems:

$$\alpha_{35}\Omega_{35}=\alpha_{8.75}\Omega_{8.75}\rightarrow d_{8.75}=d_{35}\left[\frac{35}{8.75}\frac{Z_{\rm int,35}}{Z_{\rm int,8.75}}\right]^{1/3}. \tag{29}$$

The first topic we wish to examine is the sensitivity to *beam quality* of an amplifier operating at 35 GHz comparing to an 8.75 GHz ($=\frac{35}{4}$) one. For simplicity let us assume a very strong (infinite) magnetic field guides the beam—this constraint will be released subsequently. Assuming a phase advance per cell of $2\pi/3$ ($L=2.465$ mm at 35 GHz and $L=9.86$ mm at 8.75 GHz), we can calculate the interaction impedance for four different internal radii: $R_{\rm int}=6$, 6.5, 7.0, and 7.5 mm. The corresponding result is $Z_{\rm int}(35\ \mathrm{GHz})=73$, 52, 37, and 26 Ω. Since in this particular case an ''infinite'' magnetic field is assumed, the interaction impedance quoted above is calculated by averaging the electric field experienced by all the electrons, i.e.,

$$E_{\rm eff}^2=\frac{2}{R_{\rm beam}^2}\int_0^{R_{\rm beam}}drrE_z(r)^2. \tag{30}$$

For the dynamics of this system it is sufficient to solve the 1D equations of motion with $E_{\rm eff}$ replacing E_0 and taking $\overline{r_i}=0$. In the *X*-band range the corresponding interaction impedances are $Z_{\rm int}(8.75\ \mathrm{GHz})=2700$, 2193, 1812, and 1519 Ω; these latter values are higher than generally used but they emphasize even better the difference between the two systems. For example, the significant difference in the interaction impedance emphasizes the relevance of the beam-quality question since the interaction impedance of the 35 GHz system resembles that of a free-electron laser (FEL) and the sensitivity of the latter to beam quality is a well recognized fact. A comparison of FEL and traveling-wave tube (TWT) operation can be found in Ref. [10] (p. 305).

The two frames in Fig. 1 illustrate the effect of the relative energy spread at the input on the spatial growth rate. We observe that at 35 GHz the growth rate drops to virtually zero for energy spread larger than 15% whereas at 8.75 GHz

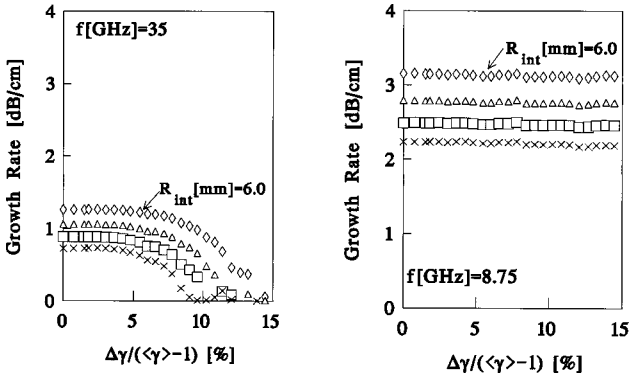

FIG. 1. Spatial growth rate of a traveling-wave amplifier as a function of the relative energy spread at the input. The internal radius of the structure is a parameter: $R_{\rm int}=6.0$, 6.5, 7.0, and 7.5 mm. The growth rate drops monotonically with $R_{\rm int}$. The left frame illustrates the performance at 35 GHz and the right one at 8.75 GHz.

there is virtually no change in this range. It should be pointed out that the system is assumed to be *uniform* and the simulation is terminated when the interaction saturates. In order to understand the reason for this sensitivity we plot in Fig. 2 the relative energy spread at the output as a function of the relative energy spread at the input. The result indicates that, since in the *X*-band system the interaction impedance is large, the energy spread at the output is also large (70%). Increasing the energy spread at the input reduces somewhat the efficiency of the interaction but the spread at the output is not even close to that at the input. This is contrary to the 35 GHz case where the interaction impedance is two orders of magnitude smaller, the energy spread at the output is much more moderate (10–20 %), and an increase to 10–15 % in the energy spread at the input reaches rapidly the value of this quantity at the output—thus the interaction efficiency is practically zero. The line in the left frame represents the case when the energy spread at the output equals that at the input. From this comparison we conclude that the sensitivity to beam quality is different in the two regimes. However, in practice this is not an obstacle in the operation of a 35 GHz traveling-wave amplifier based on a *uniform* structure and

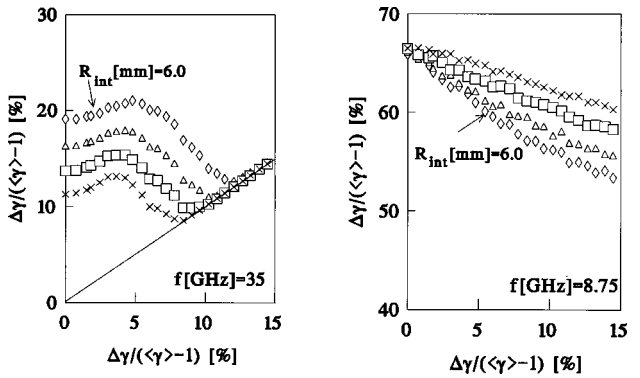

FIG. 2. Normalized energy spread at the output as a function of the relative energy spread at the input for the same conditions as in Fig. 1. As expected, the relative energy spread at the output cannot drop below its value at the input. This fact, in conjunction with the lower interaction impedance for the same $R_{\rm int}$, explains the relative sensitivity to beam quality at high frequencies.

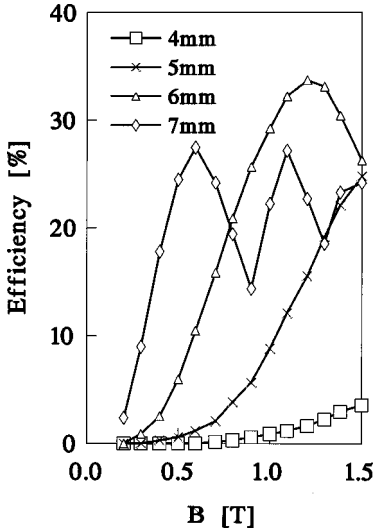

FIG. 3. The efficiency as a function of the guiding magnetic field in a tapered structure. The simulation is terminated either if electrons hit the external wall or they start to move backward; consequently, the interaction length is very short in the case of low-intensity magnetic field leading in turn to low efficiency.

''infinite'' guiding field since present technology enables us to generate a beam with a relative energy spread smaller than 5%.

Our next step is to relax the constraint of ''infinite'' guiding magnetic field of a 35 GHz amplifier but keep the relative energy spread at the input constant at 1% value. Figure 3 illustrates the efficiency in a *tapered* structure as a function of the applied magnetic field for four different disk apertures, $R_{\rm int}=4$, 5, 6, and 7 mm. In this case the simulation is terminated either if electrons hit the external wall or they start to move backward. For this reason the interaction length is very short in the case of low-intensity magnetic field and consequently the efficiency is low. According to this result, for a given internal radius (and thus interaction impedance) there is an optimal magnetic field for achieving maximum efficiency. For a 6 mm internal radius this magnetic field is slightly more than 1 T whereas for 7 mm it is about 0.5 T. It should be pointed out that in this simulation the phase velocity of the wave was tapered such that

$$\frac{1}{\beta_{\rm ph}}=\left\langle\frac{1}{\beta_i}\right\rangle_i . \tag{31}$$

This tapering keeps the average phase of all particles relative to the wave constant, i.e., $(d/d\zeta)\langle\chi_i\rangle=0$ but this is not necessarily the optimal taper.

In order to have a better understanding of the behavior as revealed in Fig. 3 let us start and examine closely the behavior of the 4 mm system. Its interaction impedance is the highest of the four and therefore the *radial* motion becomes significant close to the input and since our simulation is terminated if one particle hits the structure, the amount of energy transferred to the wave is small (low efficiency); each point along the curve corresponds to a different interaction length. For the next radius ($R_{\rm int}=5$ mm) high magnetic fields 1–1.5 T are sufficient to confine the beam and efficiency of 15–25 % is achievable before particles hit the structure. Increasing further the internal radius ($R_{\rm int}=6$ mm) reveals a similar behavior for magnetic fields smaller than 1.2 T with efficiency up to 35%. However, increasing further the magnetic field reduces the longitudinal momentum of the beam since for the same rf field the radial swing will be larger and consequently the kinetic energy available for conversion into rf is reduced and the particles slip out of phase in spite of the tapering. This behavior is even better revealed in the last case presented ($R_{\rm int}=7$ mm) where the efficiency as a function of the applied magnetic field reveals several peaks and valleys exactly as in the case of saturation.

At saturation an additional effect may contribute to this interesting behavior of the efficiency: this is a gyrotronlike interaction. In the interaction process there are sufficiently slow electrons for which instead of ''satisfying'' the regular slow wave structure resonance condition ($\omega-kv_i=0$), their radial motion enables a combined interaction which formally can be represented by $|\omega-kv_i|=\omega_c$. Such an interaction extracts energy from the rf field and transfers it to the electrons as can be concluded from the ''valleys'' in the curve corresponding to $R_{\rm int}=7$ mm. Exact description of the interaction in the vicinity of these points would require inclusion of TE modes in the analysis. In any event such a mechanism will hurt the operation of a TWT, therefore it is necessary to operate as far as possible from this regime, therefore only the first peak in the curve is of interest.

So far we examined the effect of the energy spread assuming an infinite guiding field. In addition we investigated the effect of a finite guiding field on an (initially) ideal beam. Our next step is to consider the effect of energy spread at the input on the interaction in a tapered structure which has an internal radius of 6 mm; the guiding magnetic field is 0.5 T. Figure 4 illustrates the efficiency of such a system for four different energy spreads at the input. The results are not dramatically different from those we found when the motion is assumed to be constrained to the longitudinal direction by a strong external magnetic field. As in the other case we obtain efficiencies as high as 40% in a single-stage amplifier. This

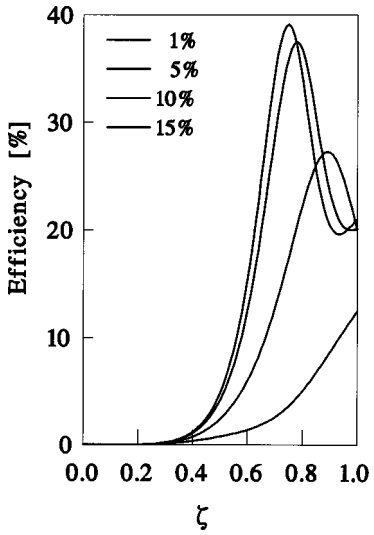

FIG. 4. The development of the efficiency in space with the relative energy spread as a parameter; $B=0.5$ T. Efficiency as high as 40% can be obtained in a single-stage amplifier.

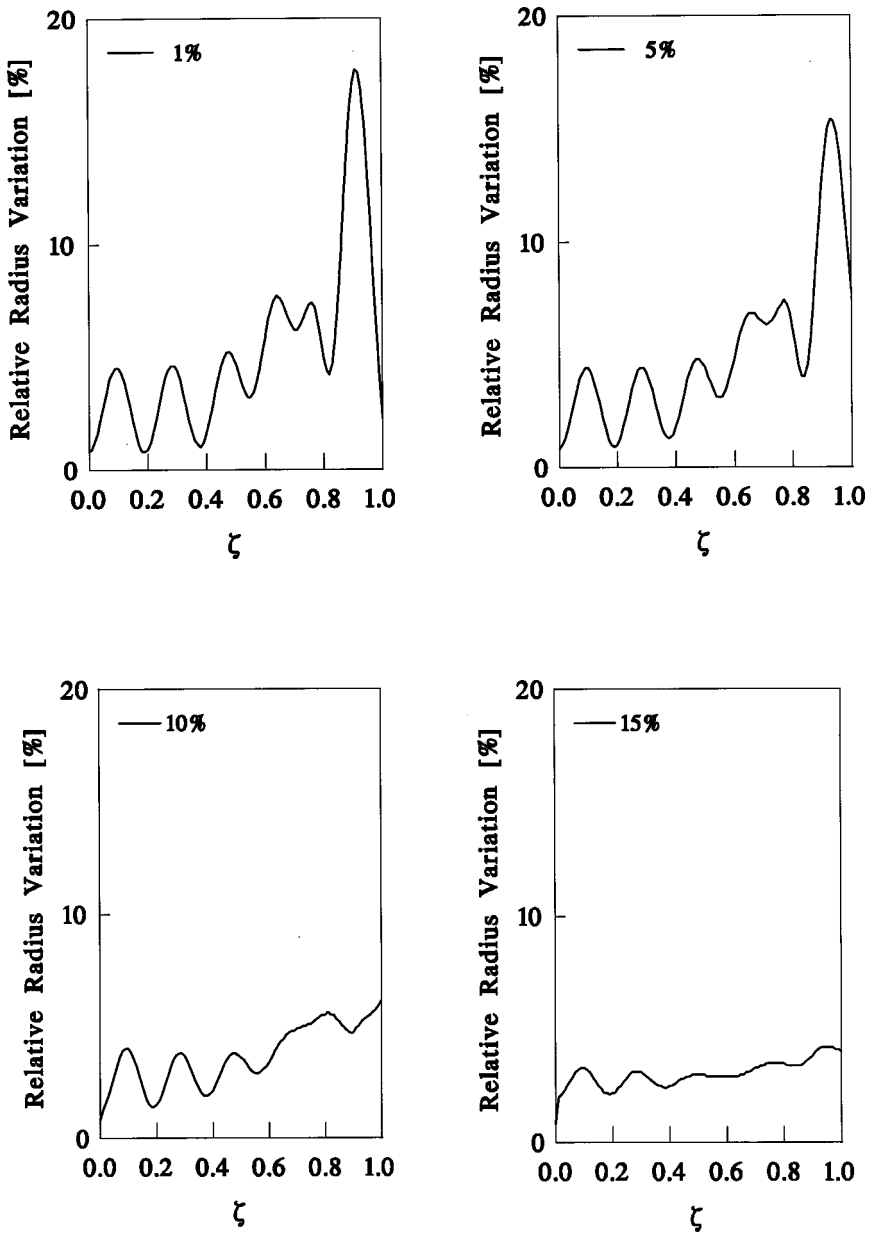

FIG. 5. The variation of the normalized radius change as it develops in the interaction region with the relative energy spread as a parameter. Note that beyond the saturation point, this normalized radius increases by a factor of more than 3 (from 5% to 15%).

may not be necessary in practice since it was found that a two-stage system can have a higher efficiency and usually the first stage is only operated at relatively low efficiency in order to bunch the beam. However, the operation of a two-stage system is beyond the scope of this study.

Figure 5 illustrates the relative change $(\Delta r/\langle r\rangle)$ in the radius of the beam which corresponds to the interaction whose efficiency is presented in Fig. 4. We find that beyond the saturation point, $\Delta r/\langle r\rangle$ increases by a factor of 3 (from 5% to 15%); this happens if the relative energy spread is less than 5%. Above 10%, the efficiency is low, which in turn implies a weak radial force and consequently the beam radius virtually does not vary.

In conclusion, a 2D quasianalytic model has been developed in order to investigate the operation of a 35 GHz traveling-wave amplifier. Based on this model we were able to establish constraints on beam quality, guiding magnetic field, and the radius of the aperture. Our main conclusions are (i) as long as the relative energy spread at the input is less than 5% the 35 GHz system should operate in a similar way as in X band; (ii) a magnetic field of 0.5 T should suffice to confine a beam which generates about 30% efficiency with a 6 mm disk aperture and a higher efficiency ($\geqslant$35%) can be achieved if a 1.2 T field is applied to a 7 mm aperture system; (iii) relative change in beam radius is confined to less than 20% even if in a single stage the efficiency approaches the 40% level.

ACKNOWLEDGMENTS

This study was supported by the U.S. Department of Energy, and by the Bi-National U.S.–Israel Science Foundation.

[1] R. D. Ruth, in *Proceedings of the Third Workshop on Pulsed RF Sources for Linear Colliders (RF'96), Shonan Village Center, Hayama, Kanagawa, Japan, April 1996*, edited by S. Fukuda (High Energy Accelerator Research Organization, 1977), p. 54.
[2] R. Palmer, SLAC Report No. SLAC-PUB-4295, 1987.
[3] P. Wilson, in *Proceedings of the Third Workshop on Pulsed RF Sources for Linear Colliders (RF'96)* (Ref. [1]), p. 9.
[4] D. U. L. Yu, J. S. Kim, and P. Wilson, in *Proceedings of the Advanced Accelerator Concepts Workshop, Port Jefferson, NY, June 1992*, edited by J. S. Wurtele, AIP Conf. Proc. No. 279 (AIP, New York, 1993),p. 85.
[5] W. Lawson, B. Hogan, J. Cheng, M. Castle, G. Saraph, J. Anderson, J. Calame, M. Reiser, and V. L. Granatstein, in *Proceedings of the Third Workshop on Pulsed RF Sources for Linear Colliders (RF'96)* (Ref. [1]), p. 225.
[6] C. Wang, J. L. Hirshfield, and A. K. Ganguly (unpublished).
[7] L. Schächter, J. A. Nation, and D. A. Shiffler, J. Appl. Phys. **70**, 114 (1991).
[8] L. Schächter and J. A. Nation, Phys. Rev. A **45**, 8820 (1992).
[9] L. Schächter, Phys. Rev. E **52**, 2037 (1995).
[10] L. Schächter, *Beam-wave Interaction in Periodic and Quasi-periodic Structures* (Springer, New York, 1996).